case of sedimentation and viscosity. The corresponding amplitudes in the Kirkwood approximation do not depend on $a$ since the hydrodynamic terms dominate the bare friction in eq 2.9. This raises the question of whether $a$-dependent amplitudes are reasonable. The approximation which we have used for the hydrodynamic **T** matrix goes beyond the Oseen approximation and incorporates $a$-dependent off-diagonal terms. Hence, even though these terms will dominate the diagonal (bare friction) terms for large N, their $a$ dependence may be reflected in $a$-dependent amplitudes. Indeed, quite generally in critical phenomena, although critical exponents are not normally sensitive to local properties, critical amplitudes usually are. Fixman has also suggested that there is a nonuniversal dependence of limiting quantities on "local" properties. His conclusions are based on dynamical simulations,[24] equilibrium simulations,[25] and simulations involving internal friction.[26] This apparent dependence is worthy of further investigation.

**Acknowledgment.** This research was financially supported, in part, by NSERC, by SERC, and by NATO (Grant RG85/0067). We acknowledge helpful conversations with Professor Raymond Kapral.

## References and Notes

(1) Zimm, B. H. *Macromolecules* **1980**, *13*, 592.
(2) See, for instance: Yamakawa, H. *Modern Theory of Polymer Solutions*; Harper and Row: New York, 1971; Chapter 6.
(3) Fixman, M. *Macromolecules* **1981**, *14*, 1706. Zimm, B. H. *Macromolecules* **1982**, *15*, 520.
(4) Wilemski, G.; Tanaka, G. *Macromolecules* **1981**, *14*, 1531. Fixman, M. *J. Chem. Phys.* **1983**, *78*, 1588.
(5) Zimm, B. H. *Macromolecules* **1984**, *17*, 795.
(6) Freire, J. J.; Prats, R.; Pla, J.; de la Torre, J. G. *Macromolecules* **1984**, *17*, 1815.
(7) Zimm, B. H. *Macromolecules* **1984**, *17*, 2441.
(8) Lipson, J. E. G.; Gaunt, D. S.; Wilkinson, M. K.; Whittington, S. G. *Macromolecules* **1987**, *20*, 186.
(9) Whittington, S. G.; Lipson, J. E. G.; Wilkinson, M. K.; Gaunt, D. S. *Macromolecules* **1986**, *19*, 1241.
(10) Rosenbluth, A. W.; Rosenbluth, M. N. *J. Chem. Phys.* **1955**, *23*, 356.
(11) Hammersley, J. M.; Morton, K. W. *J. Roy. Statist. Soc.* **1954**, *B16*, 23.
(12) Rotne, J.; Prager, S. *J. Chem. Phys.* **1969**, *50*, 4831.
(13) Felderhof, B. U. *Physica A (Amsterdam)* **1977**, *89A*, 373.
(14) Domb, C.; Gillis, J.; Wilmers, G. *Proc. Phys. Soc.* **1965**, *85*, 625.
(15) LeGuillou, J. C.; Zinn-Justin, J. *Phys. Rev. B: Condens. Matter* **1980**, *21*, 3976.
(16) Kirkwood, J. G. *J. Polym. Sci.* **1954**, *12*, 1.
(17) Huber, K.; Burchard, W.; Fetters, L. J. *Macromolecules* **1984**, *17*, 541.
(18) Stockmayer, W. H.; Fixman, M. *Ann. N. Y. Acad. Sci.* **1953**, *57*, 334.
(19) Prats, R.; Pla, J.; Friere, J. J. *Macromolecules* **1983**, *16*, 1701.
(20) de Gennes, P.-G. *Scaling Concepts in Polymer Physics*; Cornell University Press: Ithaca, NY, 1979.
(21) Rey, A.; Freire, J. J.; de la Torre, J. G. *Macromolecules* **1987**, *20*, 342.
(22) Roovers, J. E. L.; Bywater, S. *Macromolecules* **1972**, *5*, 384; **1974**, *7*, 443.
(23) Hadjichristidis, N.; Roovers, J. E. L. *J. Polym. Sci., Polym. Phys. Ed.* **1974**, *12*, 2521.
(24) Fixman, M. *Macromolecules* **1981**, *14*, 1710; *J. Chem. Phys.* **1983**, *78*, 1594.
(25) Fixman, M. *J. Chem. Phys.* **1986**, *84*, 4080.
(26) Fixman, M. *J. Chem. Phys.* **1986**, *84*, 4085.

# Attraction between Lipid Bilayer Membranes in Concentrated Solutions of Nonadsorbing Polymers: Comparison of Mean-Field Theory with Measurements of Adhesion Energy

**E. Evans* and D. Needham†**

*Departments of Pathology & Physics, University of British Columbia, Vancouver, B.C., Canada V6T 1W5, and Department of Mechanical Engineering and Material Science, Duke University, Durham, North Carolina 27706.* *Received February 19, 1987*

ABSTRACT: Recent experimental advances have made quantitation of weak membrane attraction possible in concentrated solutions of macromolecules. Here, we report direct measurements of the free energy potential for adhesion of synthetic lipid bilayers in aqueous solutions of dextran (polyglucose) over a wide range of volume fraction (0.01–0.1) and molecular weight (10 000–150 000). These polymer solutions are well-modeled by a Flory interaction parameter of 0.43, characteristic of a "good" solvent. Controlled assembly of two giant bilayer vesicles was used to evaluate the free energy potential for formation of adhesive contact. The adhesion energy for neutral (phosphatidylcholine) bilayers in 0.1 M NaCl was found to steadily increase (from 0.01 to >0.2 erg/cm$^2$) with polymer volume fraction—without any indication of a plateau—and with little dependence of polymer size. The distance dependence of the polymer-induced field was tested by incorporation of electric (phosphatidylserine) charges in the lipid bilayer surfaces to stabilize adhesion at larger membrane separations. With the use of fluorescently labeled polymer, attempts were made to measure the concentration of polymer in the gap between adherent neutral bilayers; the result was negative, which indicated a significant reduction between the surfaces. Hence, we examined a thermodynamic mean-field theory for adhesion based on interaction of surface-depletion layers. Our analysis shows that (for equilibrium exchange of the polymer between gap and bulk regions) the attractive stress on the membrane surfaces is simply the osmotic pressure reduction at the *midpoint* of the gap relative to the bulk region. Calculations of adhesion energies based on the mean-field theory agree very well with the concentration dependence of neutral bilayer adhesion for large molecular weights and with the attenuation of adhesion energy due to electric double-layer repulsion between charged bilayers in polymer solutions fixed at a specific concentration.

## Introduction

Processes that cause aggregation of cells and other membrane-bound capsules in solutions of large macromolecules are generally separated into two categories: specific and nonspecific. Specific adhesion processes involve identifiable binding reactions between suspended macromolecules and receptor molecules located at the membrane surfaces. On the other hand, nonspecific adhesion processes are not attributable to cross-binding of membrane surfaces by the suspended macromolecules.

*To whom correspondence should be sent at the University of British Columbia.
†Duke University.

0024-9297/88/2221-1822$01.50/0 

Always present are classic colloid forces that act between continuous media, i.e., van der Waals attraction, electric double-layer repulsion, and short-range structural and solvation forces.[1,2] In general, these colloidal forces simply superpose on interactions peculiar to the suspended molecules. For membranes (e.g., biological cells) with large superficial molecular structures, only electrostatic and steric repulsions are important; van der Waals attraction and short-range repulsion can be neglected. However, for lipid bilayers with small molecular head groups at the water interfaces, colloidal attraction as well as repulsion is present between surfaces. Addition of large polymers and protein macromolecules to the aqueous environment can greatly augment the weak attraction between lipid bilayers.[3,4] For dextran (polyglucose) polymers, this augmented attraction exhibits similar dependence on polymer concentration for several types of lipid head groups. Hence, it is clear that the interaction between the surfaces is nonspecific.

Two diverse conceptual views of nonspecific adhesion processes form the bases for contemporary theories that have been introduced to rationalize observations of colloidal stability and flocculation in polymer solutions.[5-7] The first view is based on adsorption and cross-bridging of the polymers between surfaces. The interaction of polymer with the surfaces is assumed to be a short-range attraction proportional to area of direct contact. Theories derived from this concept usually indicate a rapid initial rise in surface adsorption for infinitesimal volume fractions;[6,8] this is followed by a plateau with commensurate attenuation of surface–surface attraction because of excluded-volume effects in the gap between surfaces at the larger volume fractions.[6,9,10] The second—completely disparate—view of nonspecific adhesion is based on the concept that there is exclusion or depletion of polymer segments in the vicinity of the surface, i.e., no adsorption to the surfaces.[11,12] Here, theory shows that attraction is caused by interaction of the depleted concentration profiles associated with each surface which leads to a depreciated segment concentration at the center of the gap. The concentration reduction in the gap relative to the exterior bulk solution gives rise to an osmotic effect that acts to draw the surfaces together. When equilibrium exists between the gap and bulk, stabilization or approach to a plateau level is not anticipated in good solvents unless other interactions are present. The free energy potential for adhesion is expected to increase progressively with concentration even at large volume fractions. Thus, adsorption-based versus (nonadsorption) depletion-based concepts predict distinctly different adhesion properties: (i) excess polymer versus a reduction in concentration in the contact zone; (ii) rapid rise in free energy potential for adhesion at infinitesimal concentrations followed by a plateau and eventual attenuation of the attraction versus adhesion energy that progressively increases with concentration and without stabilization. Also, adsorption-based phenomena should exhibit specific dependencies on chemical attributes of the polymer segments and surface molecules whereas (nonadsorption) depletion-based processes should depend only on the colligative properties of the polymer in the solution.

Because of recent experimental advances for the study of weak bilayer interactions, it is possible to quantitate adhesion energies, test reversibility, and critically evaluate disparate theories for interactions in concentrated polymer solutions as well as in simple buffers.[3,13,14] Here, we present direct measurements of the free energy potential for adhesion of electrically neutral—and charged—lipid bilayers in solutions of dextran (polyglucose) plus 0.1 M NaCl over a wide range of volume fraction (0.01–0.1) and molecular weight (10 000–150 000). The measured values of adhesion energy were found to progressively increase with volume fraction of the polymer in solution with no indication of limitation. We also describe attempts to measure the concentration of polymer present in the gap between adherent bilayers by fluorescence assay which showed a significant reduction in polymer concentration in the gap compared to the exterior bulk solution. Based on these experimental observations, we have examined the results in the context of a self-consistent mean-field (SCMF) theory for adhesion induced by polymer depletion in the gap.

## Experimental Methods

The experimental approach is to create large bilayer capsules that can be manipulated to test surface–surface adhesivity. Lipids from two classes were used: synthetic phospholipids (1-stearoyl-2-oleoylphosphatidylcholine (SOPC) and 1-palmitoyl-2-oleoylphosphatidylserine (POPS), Avanti Biochemicals, AL) and a natural "sugar" lipid (digalactosyl diacylglycerol DGDG, Lipid Products England). These lipids were chosen to represent two types of neutral head group structures (SOPC, DGDG) and an electrically charged species (POPS). Diacyl lipids exhibit the useful feature that they spontaneously form closed vesicular capsules when hydrated from an anhydrous state. Although small in number, a few of these capsules are sufficient size (10–20 × $10^{-4}$ cm) that they can be subjected to direct micromechanical adhesion tests. Since the vesicles are formed in nonionic (sucrose or other small sugars) buffers, very small levels of surface charge are sufficient to separate lamillae and thus vesicles are usually single bilayer structures.[15] When resuspended in iso-osmotic salt solutions, the small difference in index of refraction between the interior and exterior of the vesicle greatly enhances the optical image as shown in Figure 1. Because of the extremely low solubility of lipid molecules in aqueous media, single-walled vesicles form cohesive surfaces with limited area compressibility.[14,15] Further, because of the osmotic strength of solutes trapped inside the vesicles and the small pressure differentials applied to vesicles, vesicle volumes remain constant during mechanical tests. Hence, vesicles deform as liquid-filled bags with nearly constant surface area and volume; spherical vesicles appear rigid and undeformable. Provided the surface is not forced to dilate, bilayers only oppose deformation with a very small bending rigidity.[14] For big vesicles, the bending stiffness is so small that when the vesicle is slightly deflated by osmotic increases in the exterior solution, the vesicle becomes completely flaccid and deformable. As consequences of these mechanical properties, spherical vesicles are too rigid to form adhesive contacts whereas flaccid, nonspherical vesicles easily form adhesive contacts with essentially no resistance to deformation until the surfaces are pressurized into spherical segments as shown in Figure 1.[16]

We have taken advantage of the general deformability properties of bilayer vesicles to establish a sensitive method for measurement of adhesion energy between vesicle surfaces. First, two spherical vesicles are selected and transferred from the initial suspension in a chamber on a microscope stage to an adjacent chamber which contains a slightly more concentrated buffer (0.1 M pH 7.0 phosphate buffered NaCl–PBS) plus polymer at the desired concentration. There, the vesicles rapidly deflate to new equilibrium volumes. One vesicle is aspirated by a small micropipet and held with sufficient suction to form a rigid spherical segment outside of the pipet; this forms the "test" surface for adhesion. The second vesicle is aspirated by another pipet with low suction controlled to regulate the adhesion process. The second vesicle is then maneuvered into close proximity of the test vesicle surface (Figure 1a) and the adhesion process is allowed to proceed in discrete (equilibrium) steps established by pipet suction (Figure 1b,c). This experimental procedure yields the tension in the adherent vesicle bilayer as a function of the extent of coverage of the test vesicle, both for the forward process of adhesion and the reverse process of separation. The extent of coverage $x_c$ of the test vesicle is measured by the polar height $z_c$ of the adhesion "cap" divided by the diameter $2R_s$ of the spherical

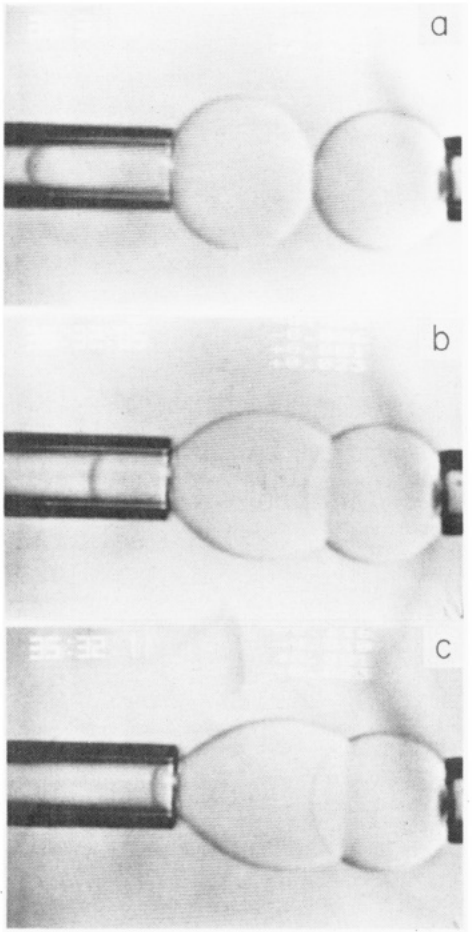


**Figure 1.** Video micrographs of a vesicle adhesion test. (a) Vesicles maneuvered into position for contact. (b,c) Adhesion configurations at equilibrium controlled by the suction pressure applied to the left-hand vesicle. Right-hand vesicle was pressurized to form a rigid spherical test surface. (Pipet caliber ~ $5 \times 10^{-4}$ cm; vesicle diameters ~ $2 \times 10^{-3}$ cm.)

test surface ($x_c = z_c/2R_s$). In the tests reported here, the adhesion was totally reversible as illustrated in Figure 2 (i.e., suction pressures that allowed contact formation were equivalent to pressures required to separate contact).

The distance scale for forces that act between bilayer surfaces is much smaller than the macroscopic dimensions observable in these experiments; thus, it is not possible to directly determine the bilayer forces. However, cumulation of the forces into an integral over distance is measurable. This integral is the negative work or free energy reduction per unit area for assembly of the bilayers from infinite separation to stable contact where the force between the surfaces is zero,

$$\gamma \equiv -\int_{\infty}^{z_g} \sigma_n \, dz \tag{1}$$

The stress $\sigma_n$ normal to the surfaces is the total action of both colloidal forces and the force induced by polymer in solution. Mechanical equilibrium in the adhesion process is established when small reductions in free energy due to formation of contact just balance small increases in mechanical work required to deform the vesicle.[17] This variational statement leads to a direct relation between the free energy potential for adhesion and the suction applied to the adherent vesicle,

$$\gamma/PR_p = f(\text{geom}) \tag{2}$$

When the product of pipet suction $P$ and radius $R_p$ is converted to tension for the adherent vesicle bilayer, this equation takes the form of the classic Young equation where the geometric factor is $(1 - \cos\theta_c)$; $\theta_c$ is the included angle between the bilayer surfaces. Because of the special mechanical and permeability properties of vesicles, the vesicle area and volume remain fixed throughout contact formation and the bilayer region exterior to the pipet forms a surface with constant mean curvature. Hence, the contact angle is a unique function of the extent of encapsulation of the spherical test surface that can be derived with a computational algorithm.[17] If the free energy potential for adhesion is uniform over the adhesion zone, then a single curve is predicted for the relationship between pipet suction and the fractional extent of coverage of the test vesicle (examples of correlation of the mechanical analysis with data from adhesion tests are shown in Figure 2).

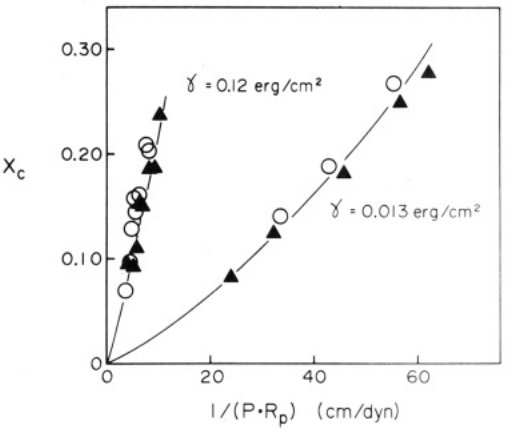


**Figure 2.** Data from two vesicle adhesion tests: fractional area $x_c$ of the rigid vesicle covered by the adherent vesicle versus the reciprocal of suction pressure $P$ multiplied by pipet radius $R_p$. Triangles (▲) represent contact formation and the open circles (O) represent separation of the contact. The curves are predictions from mechanical analysis for uniform values of adhesion energy—listed on the figure. The lower curve is for neutral SOPC vesicles in salt buffer only. The upper curve is for neutral SOPC vesicles but in salt buffer plus 9.3 g/100 cm³ dextran—36 500 $M_w$ polymer.

## Intrinsic Colloidal Forces between Bilayers

The energetics of assembly or adhesion of neutral lipid bilayers in aqueous buffer (without polymer) can be viewed conceptually as approach along a soft van der Waals attraction to a specific limit or barrier determined by the magnitude and decay of strong short-range repulsive forces.[2] This establishes a barrier to further approach at positions in the range 10–30 Å. When the bilayers contain electric charges, double-layer repulsion must be included;[1] the equilibrium contact position is displaced outward to a new location where the sum of stresses is again zero. The stress that acts normal to the bilayer surfaces is given approximately by

$$\sigma_n{}^c = -P_{sr}e^{-z_g/\lambda_{sr}} + \frac{A_H f(z_g/z_l)}{6\pi z_g{}^3} - P_{es}e^{-z_g/\lambda_{es}} \tag{3}$$

where $P_{sr}$ is the coefficient for the short-range repulsion and $\lambda_{sr}$ is the decay length; $A_H$ is the cumulative Hamaker coefficient for the van der Waals attraction, and $f_l$ is a weak retardation function of the ratio of the bilayer thickness $z_l$ to the distance between bilayers $z_g$ with a value close to unity; $P_{es}$ is the coefficient for electric double-layer repulsion, and $\lambda_{es}$ is the Debye length[1] for the decay ($\lambda_{es}$ = 9.6 Å in 0.1 M NaCl).[18]

Equilibrium separation for stable contact is established at the location where the total stress is zero. Thus, the free energy potential for assembly of the bilayers is given by the integral of the stress over the range from infinity to this location as given by eq 1. For neutral SOPC with liquid acyl chains, the adhesion energy is measured to be 0.012 erg/cm² and the bilayer separation is in the range 26–28 Å.[2,14] On the other hand, the neutral sugar-lipid DGDG exhibits a much larger adhesion energy of about 0.22 erg/cm² at a much lower separation of about 13–14

Å.[14] Also, attenuation of the adhesion energy by incorporation of fixed negative charges (POPS) into these neutral bilayers follows predictions established by classical double-layer theory.[14]

If polymer does not interact with the electric field between bilayers nor contribute significantly to the polarizability of the aqueous region between the surfaces, then these colloidal forces can be treated simply as external stresses that superpose on the action of the polymer, i.e.,

$$\sigma_n = \sigma_n^c + \sigma_n^p \tag{4}$$

Neutral dextran at volume fractions below 0.1–0.2 can be considered as an ideal, noninteracting polymer for the following reasons. Our measurements of osmotic pressure in salt buffers and distilled water show that the polymer does not interact with the monovalent salt (NaCl). Thus, there is only a negligible effect on the decay length of double-layer repulsion (due to the reduced volume fraction of water) when the polymer is present in 0.1 M NaCl solutions. Likewise, theoretical calculations show that sugar concentrations of 30% (wt/wt) do not significantly alter the van der Waals attraction between lipid bilayers.[19] Hence, we assume that the intrinsic colloidal interactions between the bilayers act as a separable external field as expressed in eq 4.

### Attraction between Surfaces due to Depletion Effects: Self-Consistent Mean-Field (SCMF) Analysis

As we will show in the Results section to follow, adhesion tests for lipid bilayer vesicles in dextran polymer solutions are consistent with the (nonadsorption) depletion type of interaction. This conclusion is based on (i) the null observation that fluorescently labeled polymer could not be detected in the gap between bilayers, (ii) the progressive increase in adhesion energy for neutral bilayers as the polymer concentration was increased to large volume fractions, and (iii) the transfer of adherent vesicle pairs with subsequent separation which showed that adhesion energy depended only on composition of the medium exterior to the contact zone. Hence, we have chosen to carefully examine depletion-based theories in conjunction with these experiments. First, we outline a simple thermodynamic approach that provides a formalism for derivation of physical stresses from the free energy of mixing and polymer configuration. The approach is based on an established mean-field approximation for the free energy density of semidilute (reasonably concentrated) polymer solutions in good solvents.

A great deal of theoretical development over the past decade or so has been designed to predict the configurations and distribution of polymer segments in the vicinity of a solid surface or between surfaces and thereby to predict the deviation of the free energy of mixing from that in the adjacent bulk region.[20-26] When the polymer solution is reasonably concentrated (in good solvent conditions) so that long-range correlations are screened by excluded-volume effects, a "constitutive" relation for the free energy density can be introduced which includes the free energy density of mixing at the local concentration (i.e., the mean-field potential) plus a term that represents free energy excess due to configurational entropy gradients.[9,11,22,27,28] The relation, called the "ground-state approximation", is deduced from a statistical equation for correlation functions of segment distribution as a self-consistent mean-field (SCMF) approximation.[11,22,28] The free energy functional for the polymer solution in the gap between bilayer surfaces is expressed by

$$F_g = A\int_0^{z_g}\left(\tilde{F} + \frac{a_m^2}{6}\left|\frac{d\psi}{dz}\right|^2\right)dz \tag{5}$$

where $\psi^2$ is the expectation value for local segment concentration, $a_m$ is the effective length of a rigid segment of the flexible polymer, $A$ is the area of the contact zone, $z$ is the local distance from one bilayer surface, and $z_g$ is the gap thickness. $\tilde{F}$ is the free energy density for mixing evaluated at the local segment concentration in the absence of gradients and given in terms of chemical potentials as

$$\tilde{F} = \frac{\upsilon\mu_p}{N_p\nu_m} + \frac{(1-\upsilon)\mu_s}{\nu_s} \tag{6}$$

or

$$\tilde{F} = \frac{\upsilon\mu_p}{N_p\nu_m} - (1-\upsilon)\pi \tag{7}$$

where $\upsilon$ is the local volume fraction of polymer segments ($\upsilon = \psi^2\nu_m$), $\mu_p$ and $\mu_s$ are chemical potentials for the polymer and solvent, $\nu_m$ and $\nu_s$ are the molecular volumes of a monomer segment and solvent, $N_p$ is the polymer index or number of segments per chain; and $\pi$ is the osmotic pressure which is proportional to the chemical potential of the solvent.[29] A more useful expression for the free energy density is in terms of the exchange chemical potential $\bar{\mu}_p$ for the polymer adjusted by the osmotic pressure work for displacement of solvent

$$\tilde{F} = \frac{\upsilon\bar{\mu}_p}{N_p\nu_m} - \pi$$

$$\frac{\bar{\mu}_p}{N_p\nu_m} \equiv \frac{\mu_p}{N_p\nu_m} + \pi = \frac{\partial\tilde{F}}{\partial\upsilon} \tag{8}$$

In the bulk region, the free energy of mixing per unit volume for the polymer solution is expressed in terms of the reference potentials,

$$\tilde{F}_B = \frac{\upsilon_B\bar{\mu}_p^B}{N_p\nu_m} - \pi_B$$

We assume that the polymer segment distribution in the gap is optimal for equilibrium at fixed gap dimensions and number of molecules in the gap. As such, the following variation defines the profile $\phi = \upsilon/\upsilon_h$ for the local volume fraction where $\upsilon_h$ is the volume fraction of segments at the midpoint of the gap:

$$\int_0^{z_g}\delta\left\{\left[\frac{\upsilon\bar{\mu}_p}{N_p\nu_m} - \pi + \frac{a_m^2}{6}\left|\frac{d\psi}{dz}\right|^2 - \lambda_c\upsilon\right]\right\}dz \equiv 0 \tag{9}$$

The Lagrange multiplier $\lambda_c$ represents a "pressure" which ensures that the constraint,

$$\bar{\upsilon}_g \equiv \frac{1}{z_g}\int_0^{z_g}\upsilon\,dz = \text{constant}$$

is satisfied appropriate to conditions for exchange of polymer between gap and bulk regions; $\bar{\upsilon}_g$ is the average volume fraction in the gap.

If we further assume that the assembly (adhesion) process is "complete" equilibrium for polymer exchange between gap and bulk regions, the variation of the total free energy with respect to mean concentration $\bar{\upsilon}_g$ in the

gap (at fixed dimensions) is identically zero as given by

$$\int_0^{z_g}\left[\frac{\upsilon(\bar{\mu}_p - \bar{\mu}_p^B)}{N_p\nu_m} + \frac{a_m^2}{6}\left|\frac{d\psi}{dz}\right|^2\right] dz \equiv 0 \qquad (10)$$

i.e., deviations of $\bar{\mu}_p$ from the exchange chemical potential for the bulk solution act as a "field" to offset free energy excess due to gradients. This embodies the essence of the (SCMF) approximation. Equation 10 for complete equilibrium is an important auxilliary equation which leads to specification of the Lagrange multiplier $\lambda_c$ as $\bar{\mu}_p^B/N_p\nu_m$. Therefore, the optimal polymer segment profile in the gap is determined from the variational statement eq 9 with this specification for $\lambda_c$

$$\int_0^{z_g}\delta\left\{\left[\frac{\upsilon(\bar{\mu}_p - \bar{\mu}_p^B)}{N_p\nu_m} - \pi + \frac{a_m^2}{6}\left|\frac{d\psi}{dz}\right|^2\right]\right\} dz = 0 \qquad (11)$$

Also, for assembly processes at complete equilibrium (between gap and bulk regions), an "excess" free energy of mixing can be expressed in terms of chemical potential differences relative to the bulk region,

$$\Delta F = A\int_0^{z_g}\left[\frac{\upsilon(\bar{\mu}_p - \bar{\mu}_p^B)}{N_p\nu_m} + (\pi_B - \pi) + \frac{a_m^2}{6}\left|\frac{d\psi}{dz}\right|^2\right] dz \qquad (12)$$

as introduced by de Gennes[9] and derived in general terms by Widom.[28] For complete equilibrium, the actual value for the "excess" free energy of mixing is

$$\Delta F = A\int_0^{z_g}(\pi_B - \pi)\, dz$$

because of eq 10. However, this relation is not a proper work potential. The derivative with respect to separation distance yields

$$\frac{1}{A}\frac{d(\Delta F)}{dz_g} = (\pi_B - \pi_h) - \int_0^{z_g}\frac{d\pi}{dz_g} dz$$

where $\pi_h$ is the osmotic pressure at the midpoint of the gap. The last term on the right-hand side is the mean-field representation of the volume × pressure differential implicit in the Gibbs excess potential, i.e.,

$$V\delta p \equiv A\int_0^{z_g}\delta(\pi_B - \pi)\, dz$$

This term must be substracted-off to obtain the differential work. When the variation of the full free energy functional is taken with respect to separation, additional terms result from eq 10. After correction for the volume × pressure differential, the complete expression specifies the work to displace the boundaries at constant surface area, i.e.,

$$\sigma_n^p\delta z_g = \delta\left\{\int_0^{z_g}\left[\frac{\upsilon(\bar{\mu}_p - \bar{\mu}_p^B)}{N_p\nu_m} + \frac{a_m^2}{6}\left|\frac{d\psi}{dz}\right|^2\right] dz\right\} + (\pi_B - \pi_h)\delta z_g$$

With eq 10, the initial term is eliminated to leave a simple result: the polymer-induced stress is the osmotic pressure reduction at the *midpoint* of the gap for complete equilibrium,

$$\sigma_n^p = \pi_B - \pi_h \qquad (13)$$

Equation 13 is analogous to the result obtained for electric double-layer forces, i.e., repulsion between electrically charged surfaces in salt solutions is *entirely* due to the excess osmotic pressure of ions at the *midpoint* of the gap.[1]

In order to determine the osmotic pressure at the midpoint of the gap, eq 11 is solved to obtain a differential equation for the optimal profile for the segment concentration in the gap,

$$\frac{a_m^2}{6}\left|\frac{d\psi}{dz}\right|^2 = \Delta\tilde{F} - \Delta\tilde{F}_h$$

$$\Delta\tilde{F} = \frac{\upsilon(\bar{\mu}_p - \bar{\mu}_p^B)}{N_p\nu_m} + (\pi_B - \pi)$$

This equation is readily integrated to give a transcendental relation between concentration $\psi_h^2$ at the midpoint of the gap and gap thickness $z_g$,

$$z_g/2 = \frac{a_m}{6^{1/2}}\int_0^{\psi_h}\frac{d\psi}{[\Delta\tilde{F} - \Delta\tilde{F}_h]^{1/2}} \qquad (14)$$

We particularize the rest of the analysis to the range of polymer concentrations dominated by second and third virial coefficients in good solvents ($\chi < 0.5$) which is valid for solutions of large dextran polymers with volume fractions 0.01–0.2. Over this range, the following approximations for chemical potential differences (evaluated at a local volume fraction in the gap minus the reference value) are derived from Flory equations as[30]

$$\frac{\upsilon(\bar{\mu}_p - \bar{\mu}_p^B)}{N_p\nu_m} \cong \left(\frac{C_\chi}{\nu_s}\right)\upsilon(\upsilon - \bar{\upsilon}_B) + \frac{\beta}{2\nu_s}\upsilon(\upsilon^2 - \bar{\upsilon}_B^2) \qquad (15)$$

$$(\pi_B - \pi) \cong \left(\frac{C_\chi}{2\nu_s}\right)(\bar{\upsilon}_B^2 - \upsilon^2) + \frac{\beta}{3\nu_s}(\bar{\upsilon}_B^3 - \upsilon^3)$$

The parameters $C_\chi$ and $\beta$ are derived from the second and third virial coefficients. In units of osmotic pressure divided by concentration squared and cubed respectively, the second and third virial coefficients are expressed as

$$kT(1 - 2\chi)/(2\rho_m^2\nu_s)$$

$$kT\beta/(3\rho_m^3\nu_s)$$

and

$$C_\chi \equiv 1 - 2\chi + \nu_s/(N_p\nu_m\bar{\upsilon}_B)$$

where $\rho_m$ is the density of the polymer in solution and $\chi$ is the Flory interaction parameter.

With these approximations and the definition $\upsilon = \psi^2\nu_m$, eq 14 for the concentration at the midpoint of the gap leads to an integral which can be evaluated as an elliptic integral (see Appendix I),

$$z_g/2 = \frac{\zeta_m}{A_v^{1/2}}\int_0^1\frac{d\tilde{\psi}}{[(1 - \tilde{\psi}^2)(1 - B_v\tilde{\psi}^2 - C_v\tilde{\psi}^4)]^{1/2}} \qquad (16)$$

Equation 16 has been scaled to obtain a universal form in terms of dimensionless parameters,

$$\tilde{\psi} \equiv \psi/\psi_h$$

$$A_v \equiv 1 - \frac{\upsilon_h}{2\bar{\upsilon}_B} + \frac{\beta\bar{\upsilon}_B}{2C_\chi}\left[1 - \frac{\upsilon_h^2}{3\bar{\upsilon}_B^2}\right]$$

$$B_v \equiv \frac{\upsilon_h}{2\bar{\upsilon}_B A_v}\left[1 + \frac{\beta\upsilon_h}{3C_\chi}\right]$$

$$C_v \equiv \frac{\beta v_h^2}{6C_\chi \bar{v}_B A_v} \tag{17}$$

Gap positions and thickness are scaled by a characteristic length $\zeta_m$, which represents the depletion zone adjacent to each surface and the decay of depletion with distance,

$$\zeta_m \equiv a_m \left[ \frac{\nu_s}{6\nu_m \bar{v}_B C_\chi} \right]^{1/2} \tag{18}$$

Hence, the volume fraction $v_h$ at the center of the gap is specified along with the normal stress $\sigma_n^p$ induced by the polymer.

With exception of the polymer segment length $a_m$, all of the parameters in the mean-field theory are physical-chemical properties known a priori with reasonable certainty: i.e., $\nu_m$ and $\nu_s$ are obtained from densities and molecular weights;[31] $N_p$, $\chi$, and $\beta$ are calculated from virial coefficients (e.g., measured by osmotic pressure); the volume fraction in the bulk region $\bar{v}_B$ is the concentration divided by density ($\rho_m$ = 1.64 gm/cm$^3$ for dextran in solution). On the other hand, the effective polymer segment length or monomer size $a_m$ is expected to be on the order of $\nu_m^{1/3}$ but can only be deduced from radius of gyration measurements and theoretical prescriptions based on polymer statistics. Because of the inherent uncertainty in $a_m$ (range 6–9 Å),[32] it can be regarded as a weakly adjustable parameter in the calculations which follow in the Results section.

## Results: Adhesion Studies in Dextran Solutions

Sharp-cut dextran fractions were provided by a gracious gift from Dr. K. Granath (Pharmacia, Sweden) through our colleague Dr. D. E. Brooks (University of British Columbia). Three fractions were used, identified as 11 200, 36 500, and 147 500 weight-average molecular weights with ratios of weight-average $M_w$ to number-average $M_n$ molecular weights of 2.07, 1.34, and 1.56, respectively. For solutions of these fractions up to 10% by volume, osmotic pressures were measured by freezing point depression and checked by vapor pressure osmometry at high concentration. Results are plotted in Figure 3. The second virial coefficients (listed in Table I) were derived from the osmotic pressure data for all fractions. Only the first virial coefficient of the low molecular weight fraction could be established from osmotic pressure data.[33] The number-average molecular weights were 3400, 27 200, and 94 300 for these fractions. The Flory interaction parameter which characterizes the quality of the solvent (derived from the second virial coefficient) was found to be 0.428, i.e., in the "good" solvent range. No third virial coefficient was required for volume fractions less than 0.1.

Micromechanical adhesion tests were performed with 5–10 neutral (SOPC) vesicle pairs at each polymer concentration in the range of 1–15 g/100 cm$^3$ (wt/vol). These results are plotted in Figure 4 as a function of volume fraction ($\bar{v}_B$ = 0.611 wt/vol). Since the vesicle surfaces were uncharged, there was a threshold level of adhesion energy (0.01 erg/cm$^2$) caused by van der Waals attraction, i.e., the free energy potential at zero concentration. As the polymer concentration in solution was increased, adhesion energies increased progressively (from 0.01 to >0.2 erg/cm$^2$) with no tendency to plateau or saturate and with essentially no dependence on polymer size. To test the effect of molecular composition of the neutral surface, the free energy potential for adhesion of sugar-lipid (DGDG) vesicles was measured in solutions of 9.3 g/100 cm$^3$ dextran (both 147 500 and 36 500 fractions) for comparison with the

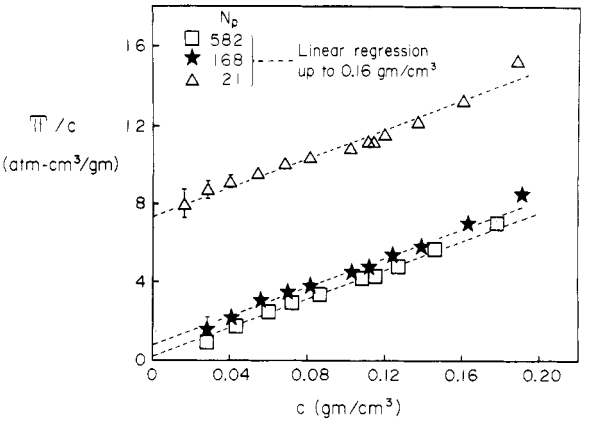


**Figure 3.** Measurements of osmotic pressure divided by polymer concentration (wt/vol) plotted versus concentration. The intercept and slope provide measures of the first and second virial coefficients for the three dextran fractions (△) 11 200, (★) 36 500, (□) 147 500 $M_w$.

**Table I**
**First and Second Virial Coefficients, Interaction Parameter, and Number-Average Molecular Weight for Osmotic Pressure Data (Figure 3)**

| dextran fractn, MW | first virial coeff,[33] atm cm$^3$/g | second virial coeff, atm cm$^3$/g$^2$ | no.-av. molecular wt.[33] ($M_n$) | Flory interaction param ($\chi$) |
|---|---|---|---|---|
| 11 200 | 7.30 | 36.3 | 3 330 | 0.428 |
| 36 500 | 0.893 | 36.3 | 27 200 | 0.428 |
| 147 500 | 0.258 | 36.3 | 94 300 | 0.428 |

measurements at the same concentration with the neutral SOPC vesicles. Adhesion energies for the DGDG vesicles in both dextrans were 0.4 erg/cm$^2$, clearly much stronger than for the SOPC vesicles (0.13 erg/cm$^2$). However, the differential-adhesion energies (in excess of the baseline van der Waals attraction potential—0.22 erg/cm$^2$ for DGDG) were comparable for these neutral lipids. This demonstrates the nonspecific character of the adhesion process, i.e., no recognizable dependence on surface composition. (The slightly greater differential-adhesion energy for DGDG vesicles can be accounted for by inclusion of the additional energy to displace the polymer-induced stress from separations of 27 Å for SOPC to 13 Å for DGDG.)

To test the dependence of adhesion energy on final gap separation, electrically charged (SOPC + POPS) bilayer vesicles were assembled in dextran solutions fixed at 9.3 g/100 cm$^3$ plus 0.1 M NaCl. Attenuation of adhesion energy as a function of surface charge concentration is shown in Figure 5. Unlike the behavior of the adhesion energy for neutral lipid bilayers, there was an obvious difference between the small and higher molecular weight polymers. Adhesion could be prevented by surface charge contents greater than 15 mol % POPS in solutions of the small molecular weight polymer; but even for POPS concentrations in excess of 30 mol%, there was a measurable level of adhesion between vesicles with the higher molecular weight polymers. The latter result clearly shows the long-range action of the polymer-induced attraction.

Based on measured virial coefficients, Figure 6 shows the predictions of stress from the SCMF analysis (eq 13) versus separation for bilayers in dextran solutions of 0.01 and 0.1 volume fractions. Also, calculations of the intrinsic colloidal stresses (eq 3) for neutral SOPC bilayers are plotted in Figure 6 based on data described in ref 14. Equilibrium separation is defined by zero *total* stress; hence, the gap is reduced slightly from 27 to 24 Å at the higher polymer concentration. Integration of the total

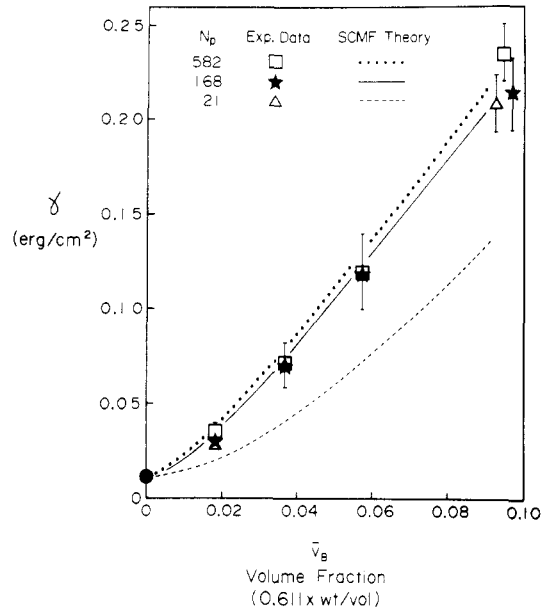


**Figure 4.** Adhesion energies (erg/cm$^2$) for neutral SOPC bilayers in 0.1 M salt (PBS) plus dextran polymer at volume fractions up to 0.1. Results are given for the three polymer fractions represented by number-average polymer indices, $N_p$ (i.e., equivalent number of glucose monomers). The curves are predictions obtained from self-consistent, mean-field theory (discussed in text).

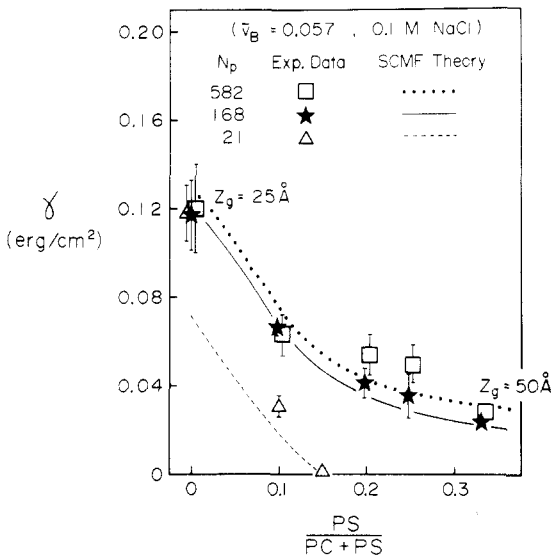


**Figure 5.** Adhesion energies (erg/cm$^2$) for charged bilayers in 0.1 M salt (PBS) plus dextran polymer—*fixed at a volume fraction* of 0.057 (9.3 g/100 cm$^3$)—versus charge content given by composition POPS/(POPS + SOPC). Again, curves are predictions obtained from self-consistent, mean-field theory (discussed in text) in conjunction with stabilization of adhesion at larger separations by electric double-layer repulsion.

stress (eq 4) from infinity to equilibrium separation yields the free energy reduction per unit area—or adhesion energy (eq 1). Predictions for adhesion energy are plotted in Figure 4 along with the direct measurements. (Note: a fixed value of 6.5 Å was used for $a_m$ in all calculations; this is $1.2\nu_m^{1/3}$, well within the range of values for segment length in the literature.[32]) Even though the approximations embodied in SCMF approach were not expected to work, we have calculated the interaction potential for the small dextran polymer ($N_p$ = 21), also plotted in Figure 4. Similarly, the adhesion energy was calculated for DGDG bilayers in dextran solutions at a fixed concentration of 9.3 g/cm$^3$. The result was 0.39 erg/cm$^2$ as compared with the measured value of 0.4 erg/cm$^2$. Here, the polymer-

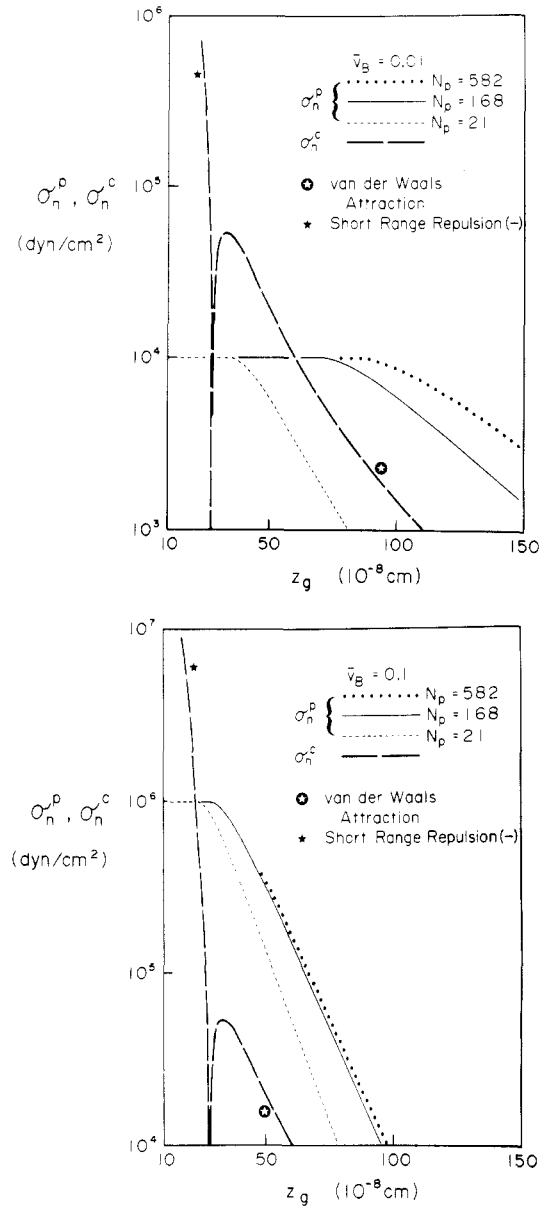


**Figure 6.** Predictions of attractive stresses induced by nonadsorbant polymers in good solvents and the stress for intrinsic colloidal attraction/repulsion between neutral bilayers versus separation. (a, top) Polymer volume fraction of 0.01; (b, bottom) volume fraction of 0.1 (note the order of magnitude change in scale).

induced attraction includes the same free energy reduction per unit area as for SOPC bilayers plus an added reduction given by the osmotic pressure multiplied by the gap displacement from 24 Å down to 13 Å (since theory predicts complete exclusion of polymer from the gap below 30 Å).

We have also calculated the attenuation of adhesion energy for the negatively charged surfaces (SOPC + POPS) at fixed polymer concentration by including the electric double-layer stresses. The stress coefficient $P_{es}$ for double-layer repulsion was calculated from the nonlinear Poisson–Boltzmann relations and Guoy–Chapman theory[1] as a function of PS content; the well-established binding[34] of $Na^+$ to PS was modeled by an equilibrium constant $K_{Na^+}$ = 0.6 M$^{-1}$. SCMF predictions for adhesion energies in solutions of each polymer fraction fixed at 9.3 g/100 cm$^3$ ($\bar{v}_B$ = 0.057) are plotted in Figure 5. Also, the values obtained for equilibrium separation from these calculations are noted in Figure 5, which shows stabilization of the gap at larger separations as surface charge is increased.

In order to verify the depletion hypothesis, we carried out two additional sets of experiments. In the first set of experiments, we performed the following sequence of vesicle adhesion–separation tests: an adherent vesicle pair was first assembled in the salt buffer without polymer where adhesive contact was established by van der Waals attraction. The adherent pair was transferred within a few seconds (with care so as not to disrupt the contact) to an adjacent chamber that contained a high concentration of polymer (~5 g/100 cm$^3$). The adhesion energy was then measured by separation of the contact in the final solution. Likewise, an adherent vesicle pair was first assembled in a solution with polymer and then transferred to the pure salt buffer without disruption of the contact; again the adhesion energy was measured by separation in the final solution. The rationale behind these tests was the expectation that macromolecules would be prevented from entering the gap (via the first procedure) or be trapped in the gap (by the second procedure) because of kinetic restrictions. Thus if polymer cross-bridges were involved in adhesion, the measured values for energy should have been determined primarily by the composition of the initial solution in which adhesion was first established. However, in both tests, the adhesion energies at separation were identical with values determined for reversible assembly and separation in solutions of composition equivalent to that of the *final* test medium.

In the second set of experiments, we attempted to directly quantitate the number of polymer molecules captured in the gap between adherent surfaces. The procedure involved formation of an adherent vesicle pair in a solution that continued fluorescently labeled dextran polymer (150 000 $M_w$) at 5 g/100 cm$^3$ concentration, followed by transfer of the adherent pair to an adjacent chamber that contained the same concentration of polymer but without fluorescent label. Since the vesicles did not separate, it was expected that fluorescent polymer trapped in the adhesion zone would be detectable over a long time period until diminished by exchange diffusion with the exterior solution. The results were negative; we could not detect any fluorescence in the contact zone except at the unusual location where there was an obvious invagination formed by liquid trapped during the adhesion process.[35] Based on dimensions of $5 \times 10^{-6}$ cm as an estimate of the minimum gap thickness and the bulk concentration of polymer, fluorescence should have easily been detected with our photometric system down to 10% of the bulk concentration. This observation clearly showed that there was not an excess of polymer in the gap but rather a significant reduction in comparison to the bulk concentration.

## Conclusions and Discussion

Self-consistent mean-field theory for large nonadsorbent polymers in good solvents agrees very well with our direct measurements of adhesion energy for neutral lipid bilayers. The attractive potential due to polymer in solution is predicted to be the integral (from large separation to stable contact) of the osmotic pressure reduction at the *midpoint* of the gap; the reduction arises from interaction of depletion layers associated with each surface. Values for adhesion energy are calculated directly from measured colligative properties of the polymer in solution with inclusion of the established colloidal attraction between bilayers in the absence of polymer. The only adjustable parameter is the segment length or monomer size which must be close to values deduced from measurements of radius of gyration and theoretical predictions of polymer configuration in dilute solution. Hence, this parameter can vary only over a small range and, once chosen, is *fixed* for all correlations. The (SCMF) theory also correlates well with the attenuation of adhesion energy measured for charged surfaces in solutions of fixed polymer concentration which implies that it is a good model for the distance dependence of the polymer-induced field. The theory does not work well for the small polymer whose characteristics do not satisfy the approximations used in the analysis. This is most likely because the theoretical prediction for stress neglects the contribution from the first virial coefficient in the osmotic pressure. Also, the small polymer fraction was highly polydisperse which may account for the similarity to the results with the larger $M_w$ fractions.

The (SCMF) model presented here is similar to the approach of Joanny et al.[11] except the analysis has been extended to include explicit treatments of the equilibrium exchange of polymer between gap and bulk regions and derivation of a work potential. In the approach of Joanny et al., the interaction potential is given by

$$z_g < 4\zeta_m \qquad \Delta F/A \simeq 3.78\pi_B\zeta_m(1 - z_g/4\zeta_m) \quad (19)$$

where the characteristic depletion length $\zeta_m$ is the same[36] as that defined in eq 18. Equation 19 is a close approximation to the actual free energy relation

$$\Delta F/A = -\int_0^{z_g}(\pi_B - \pi)\, dz + \text{constant} \quad (20)$$

for equilibrium exchange of the polymer between gap and bulk regions. Likewise, Fleer et al.[12] used a mean-field lattice model to compute interaction energies and depletion scales for nonadsorbing polymers. Their results yielded an empirical relation similar to that of Joanny et al.[11]

$$z_g < 2\zeta_m^{FSV} \qquad \Delta F/A \simeq 2\pi_B\zeta_m^{FSV}(1 - z_g/2\zeta_m^{FSV}) \quad (21)$$

Here, the characteristic scale for depletion $\zeta_m^{FSV}$ is slightly different and was found by computational analysis to be[12]

$$\zeta_m^{FSV} \simeq \frac{\pi a_m}{4}\left[\frac{\nu_s}{\nu_m c_\chi \bar{v}_B}\right]^{1/2} - \frac{a_m}{2}$$

for large polymers in good solvent conditions.[36] The (SCMF) analysis described in this paper as well as those in ref 11 and 12 yield adhesion energy coefficients that scale as osmotic pressure multiplied by depletion length to give the same dependence on volume fraction, $\bar{v}_B^{3/2}$. Indeed, this dependence on volume fraction is also obtained with more general scaling theories where the power-law dependence of chemical potentials on volume fraction deviates from ideal Flory relations.[9,25]

Direct comparison of the results from ref 11 and 12 with the predictions of this analysis (eq 13 and 1), however, shows systematic differences in the concentration dependence of neutral bilayer adhesion, Figure 7a. The differences result because the derivative of eq 20 with distance at constant area is not the osmotic pressure reduction at the midpoint of the gap as discussed previously. The major difference between derivations shows up in the decay with gap separation. The stress defined by the osmotic pressure reduction at the midpoint of the gap decays much slower than the stress defined by the change in free energy, eq 20, with separation. The latter derivative yields a steplike increase to the bulk osmotic pressure below separations where the depletion layers of each surface intersect. The different ranges for these stress derivations are apparent in correlations of adhesion energy versus charged lipid content in polymer solutions of fixed concentration, Figure 7b. The attenuation of adhesion energy with increased surface charge content is predicted to be very precipitous

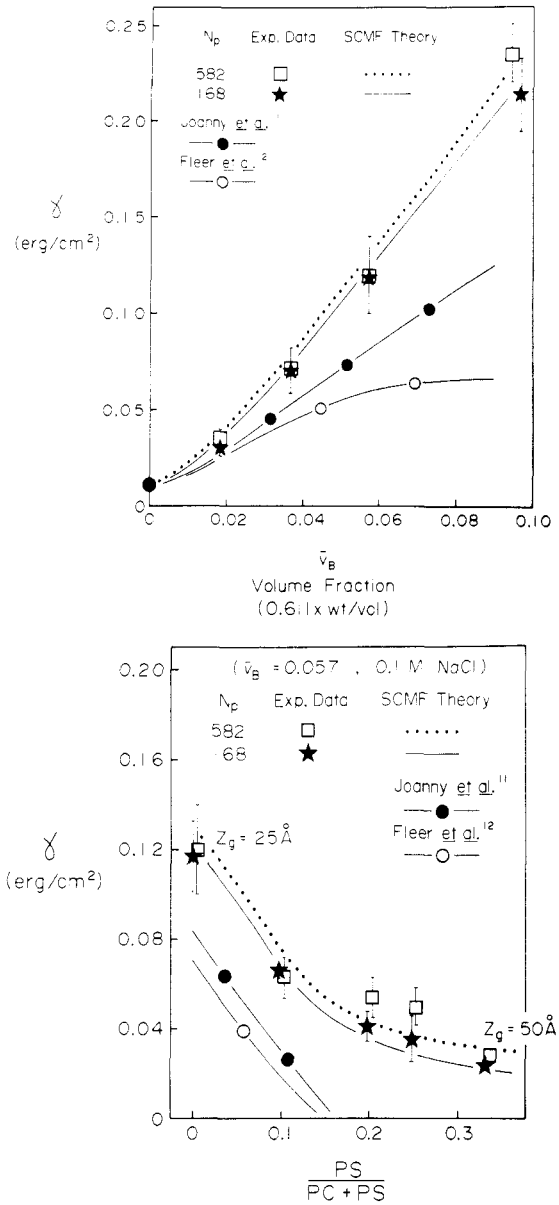


**Figure 7.** Comparison of predictions for depletion-based attraction with measurements of adhesion energy in solutions of large dextran polymers. (a, top) Neutral phosphatidylcholine bilayer adhesion as a function of volume fraction of polymer in solution. (b, bottom) Electrically charged bilayer adhesion in solutions of fixed polymer concentration ($\bar{v}_B$ = 0.057) as a function of surface charge content. Symbols: Measured values of adhesion energy (★ and □); continuous solid and dotted lines (SCMF) are predictions from this analysis; solid line with closed circles is prediction from ref 11; solid line with open circles is prediction from ref 12.

for the models in ref 11 and 12 because of the much shorter range depletion forces. Clearly, the experimental measurements correlate well with the long-range decay of the osmotic pressure reduction at the midpoint of the gap.

Another model introduced by Feigin and Napper[37] predicts different phenomenological behavior. Their model predicts a repulsive barrier at large separations before attraction at closer range. The values of the repulsive barrier indicated in their analysis would be on the order of 0.04 erg/cm² which would preclude adhesion. We have found no evidence of any repulsion in our adhesion measurements with neutral systems. Finally, Luckham and Klein[38] proposed an empirical relation for the interaction potential similar to the result derived in our analysis. In their elegant measurements of the force as a function of distance between curved mica sheets, they were unable to verify this relation in a nonadsorbent polymer (polystyrene in toluene) solution because of the limitation on force detection and volume fraction in their experiments. This demonstrates a very useful aspect of vesicle adhesion experiments; i.e., weak interactions can be measured in concentrated solutions of macromolecules. We are currently measuring adhesion energies between lipid bilayers in PEO solutions over the range of volume fractions from 0.01 to 0.1. The behavior is similar to that in dextran solutions but much stronger because of the larger second and third virial coefficients for PEO in aqueous solution.

**Acknowledgment.** This work was supported by the Medical Research Council of Canada through Grant MT 7477. E.A.E. is grateful to the Alexander von Humboldt Foundation, Federal Republic of Germany, for a Senior Scientist Award.

## Appendix I. Transcendental Equation for Concentration at Midpoint of Gap

The transcendental relation between concentration at the midpoint of the gap and the gap thickness is given by the dimensionless integral eq 16,

$$z_g/2 = \frac{\zeta_m}{A_v^{1/2}} \int_0^1 \frac{d\tilde{\psi}}{[(1-\tilde{\psi}^2)(1-B_v\tilde{\psi}^2-C_v\tilde{\psi}^4)]^{1/2}}$$

Based on the properties of complete elliptic integrals,[39] this universal integral reduces to

$$z_g/(2\zeta_m A_v^{1/2}) = K\left(\frac{a+b}{1+b}\right) \Big/ (1+b)^{1/2}$$

where

$$K(y) \equiv \int_0^{\pi/2} \frac{d\theta}{[1-y\sin^2\theta]^{1/2}}$$

$$a \equiv \frac{(B_v^2+4C_v)^{1/2}+B_v}{2}$$

$$b \equiv \frac{(B_v^2+4C_v)^{1/2}-B_v}{2}$$

## List of Symbols

| | |
|---|---|
| $a_m$ | polymer segment or monomer length (cm) |
| $A$ | area of surface–surface contact (cm²) |
| $A_H$ | Hamaker coefficient for van der Waals attraction (erg) |
| $B$ | membrane elastic bending modulus (erg) |
| $\beta$ | dimensionless form of the third virial coefficient |
| $\chi$ | Flory parameter for solvent quality ($\chi < 0.5 \Rightarrow$ good solvent) |
| $C_\chi$ | dimensionless form of the second virial coefficient |
| $F, F_g, F_B$ | free energy of mixing: total, in gap between surfaces, in bulk region (kT units) |
| $\tilde{F}$ | local free energy of mixing per unit volume (in units of kT/volume) |
| $\gamma$ | free energy reduction per unit area of contact formation, adhesion energy per unit area (erg/cm²) |
| $kT$ | Boltzmann constant multiplied by temperature ($\simeq 4.1 \times 10^{-14}$ erg) |
| $\lambda_c$ | Lagrange multiplier chosen to satisfy the nature of polymer exchange between gap and bulk regions; i.e., equilibrium or restricted |
| $\lambda_{sr}, \lambda_{es}$ | characteristic decay lengths for intrinsic short-range solvation forces and long-range electric double-layer forces between bilayer membranes (cm) |

$M_n$, $M_w$ number-average and weight-average molecular weights for the polymer fractions (g/mol)
$\mu_p$, $\mu_s$ chemical potentials (in units of kT/molecule) relative to standard state (of each pure component) for polymer and solvent
$\bar{\mu}_p$, $\bar{\mu}_p^B$ exchange chemical potentials (in units of kT/molecule) of polymer: at a local position in gap, in bulk region
$N_A$ Avogadro's number
$N_p$, $\tilde{N}_p$ number-average polymer index (average number of segments/polymer); polymer index scaled by ratio of monomer volume to solvent volume
$\nu_m$, $\nu_s$ volumes ($cm^3$) for a polymer segment (monomer) and a solvent molecule, respectively
$P$ pipet suction pressure ($dyn/cm^2$)
$P_{sr}$, $P_{es}$ pressure coefficients for intrinsic short-range solvation forces and long-range electric double-layer forces between bilayer membranes ($dyn/cm^2$)
$\phi$ ratio of local monomer concentration to concentration at midpoint of gap between surfaces
$\pi$, $\pi_h$, $\pi_B$ osmotic pressures ($dyn/cm^2$): at a local position in the gap, at the midpoint of the gap, and in the bulk region
$\psi^2$, $\psi_h^2$, $\tilde{\psi}^2$ expectation value for concentration ($g/cm^3$) of polymer segments: at specific position in gap, at midpoint of gap, ratio of local concentration to concentration at midpoint
$\rho_m$, $\rho_s$ densities ($g/cm^3$): polymer in solution, solvent
$R_p$, $R_s$ pipet radius; spherical radius of pressurized test-vesicle surface (cm)
$r_c$ radius of contact circle formed at boundary of adhesion zone (cm)
$\sigma_n$, $\sigma_n^c$, $\sigma_n^p$ stress ($dyn/cm^2$) normal to the membrane surfaces, positive in the sense of the normal into the gap: total stress, intrinsic colloidal stress, added stress due to polymer in solution
$\theta_c$ included angle between membrane surfaces at the edge of the contact zone
$\upsilon$, $\upsilon_h$, $\bar{\upsilon}_g$, $\bar{\upsilon}_B$ volume fraction of polymer segments: at local point in gap, at midpoint of gap, average over gap, average over bulk region
$V_g$, $V_B$ volumes of gap and bulk regions ($cm^3$)
$x_c$ fractional coverage of pressurized test-vesicle surface
$z_c$ height (cm) of spherical membrane cap (segment) which adheres to pressurized test-vesicle surface
$z$, $z_g$ position in the gap measured as distance from one surface: at a local point, total gap thickness
$\zeta_m$ characteristic thickness for depletion layer (cm)

**Registry No.** SOPC, 6753-56-6; POPS, 79980-16-8; dextran, 9004-54-0.

## References and Notes


(1) Verwey, E. J. W.; Overbeek, J. Th. G. *Theory of the Stability of Lyophobic Colloids*; Elsevier: Amsterdam, 1948.
(2) Parsegian, V. A.; Fuller, N.; Rand, R. P. *Proc. Natl. Acad. Sci. U.S.A.* **1979**, *76*, 2750.
(3) Evans, E.; Metcalfe, M. *Biophys. J.* **1984**, *45*, 715.
(4) Evans, E.; Needham, D.; Janzen, J. In *Proteins at Interfaces*; Brash, J., Horbett, T., Eds.; American Chemical Society: Washington, DC, 1987; p 88.
(5) Tadros, Th. F. In *Polymer Colloids*; Buscall, R., Corner, T., Stageman, J. F., Eds.; Elsevier Applied Science: London, 1985; p 105.
(6) Vincent, B. In *Polymer Adsorption and Dispersion Stability*; Goddard, E. D., Vincent, B., Eds.; American Chemical Society: Washington, DC, 1984; p 1.
(7) Napper, D. H. *Polymeric Stabilization of Colloidal Dispersions*; Academic: London, 1983.
(8) de Gennes, P.-G. *J. Phys. (Les Ulis, Fr.)* **1976**, *37*, 1445.
(9) de Gennes, P.-G. *Macromolecules* **1982**, *15*, 492.
(10) Scheutjens, J. M. H. M.; Fleer, G. J. *Macromolecules* **1985**, *18*, 1982.
(11) Joanny, J. F.; Leibler, L.; de Gennes, P.-G. *J. Polym. Sci., Polym. Phys. Ed.* **1979**, *17*, 1073.
(12) Fleer, G. J.; Scheutjens, J. M. H. M.; Vincent, B. In *Polymer Adsorption and Dispersion Stability*; Goddard, E. D., Vincent, B., Eds.; American Chemical Society: Washington, DC, 1984; p 245.
(13) Evans, E.; Metcalfe, M. *Biophys. J.* **1984**, *46*, 423.
(14) Evans, E.; Needham, D. *J. Phys. Chem.* **1987**, *91*, 4219.
(15) Kwok, R.; Evans, E. *Biophys. J.* **1981**, *35*, 637.
(16) The small bending rigidity (represented by the elastic modulus $B \simeq 10^{-12}$ erg) only produces a small edge energy effect at the sharp bend where the membrane adheres to the other surface. The fractional correction due to the edge energy is approximately $(B/\gamma \cdot r_c^2)^{1/2}$, where $\gamma$ is the energy per unit area of adhesive contact formation and $r_c$ is the radius of the contact circle. Even for the lowest levels of adhesion energy studied here, this effect is only a few percent.
(17) Evans, E. *Biophys. J.* **1980**, *31*, 425.
(18) The interactions listed in eq 3 are given as functions of the same separation distance; however, the actual origin for each interaction is difficult to define because of molecular motion and architecture. The "mass-average" water gap $z_g$ between bilayers is a good choice when separations are large compared to the surface molecular "roughness" scale.
(19) Parsegian, V. A. *Annu. Rev. Biophys. Bioeng.* **1973**, *2*, 221.
(20) Mackor, E.; van der Waals, J. *J. Colloid Sci.* **1952**, *7*, 535.
(21) Ash, S.; Findenegg, G. *Trans. Faraday Soc.* **1971**, *67*, 2122.
(22) Edwards, S. F. *Proc. Phys. Soc., London* **1965**, *85*, 613.
(23) Silberberg, A. *J. Chem. Phys.* **1967**, *46*, 1105; **1968**, *48*, 2835.
(24) Roe, R. J. *J. Chem. Phys.* **1974**, *60*, 4192.
(25) de Gennes, P.-G. *Scaling Concepts in Polymer Physics*; Cornell University Press: Ithaca, NY, 1979.
(26) Scheutjens, J. M. H. M.; Fleer, G. F. *Adv. Colloid Interface Sci.* **1982**, *16*, 361; **1983**, *18*, 309.
(27) Cahn, J. W.; Hilliard, J. E. *J. Chem. Phys.* **1958**, *28*, 258.
(28) Widom, G. *Physica A: (Amsterdam)* **1979**, *95A*, 1.
(29) Note: chemical potentials and free energies are assumed to be in units of thermal energy, i.e., normalized by $kT \simeq 4.1 \times 10^{-14}$ erg.
(30) Flory, P. J. *Principles of Polymer Chemistry*; Cornell University Press, Ithaca, NY, 1953.
(31) Note: For dextran and water, $\nu_s = 29.9 \times 10^{-24}$ $cm^3$; $\nu_m = 164.0 \times 10^{-24}$ $cm^3$; $N_p = M_n/162$.
(32) Granath, K. A. *J. Colloid Interface Sci.* **1958**, *13*, 308.
(33) The number-average molecular weights for the larger 36 500 and 147 500 $M_w$ fractions could not be accurately measured by osmotic pressure methods. The values given in Table I for the first virial coefficients of these fractions are those measured by Dr. Granath which provide the intercepts at zero concentration in Figure 3.
(34) Eisenberg, M.; Gresalfi, T.; Riccio, T.; McLaughlin, S. *Biochemistry* **1979**, *18*, 3213.
(35) Trapped liquid regions were not formed when the vesicles were assembled carefully by slow discrete steps; the contact zone appeared uniformly thin in optical thickness.
(36) When comparing various analyses, it is essential to recognize that derivations based on definition of equal monomer and solvent volumes ($\nu_m$, $\nu_s$) must be rescaled in the following way: excluded volume $\times$ $\nu_m/\nu_s$ and $N_p \times \nu_m/\nu_s$.
(37) Feigin, R. I.; Napper, D. H. *J. Colloid Interface Sci.* **1980**, *75*, 525.
(38) Luckham, P. F.; Klein, J. *Macromolecules* **1985**, *18*, 721.
(39) Abramowitz, M.; Stegun, I. A. *Handbook of Mathematical Functions*; Dover Publications: New York, 1965.